

# Spin Chains and Electron Transfer at Stepped Silicon Surfaces

J. Aulbach<sup>1</sup>, S. C. Erwin<sup>2</sup>, R. Claessen<sup>1</sup> and J. Schäfer<sup>1</sup>

<sup>1</sup>*Physikalisches Institut und Röntgen Center for Complex Material Systems (RCCM),  
Universität Würzburg, D-97074 Würzburg, Germany*

<sup>2</sup>*Center for Computational Materials Science, Naval Research Laboratory, Washington, DC 20375, USA*

High-index surfaces of silicon with adsorbed gold can reconstruct to form highly ordered linear step arrays. These steps take the form of a narrow strip of graphitic silicon. In some cases—specifically, for Si(553)-Au and Si(557)-Au—a large fraction of the silicon atoms at the exposed edge of this strip are known to be spin-polarized and charge-ordered along the edge. The periodicity of this charge ordering is always commensurate with the structural periodicity along the step edge and hence leads to highly ordered arrays of local magnetic moments that can be regarded as “spin chains.” Here, we demonstrate theoretically as well as experimentally that the closely related Si(775)-Au surface has—despite its very similar overall structure—zero spin polarization at its step edge. Using a combination of density-functional theory and scanning tunneling microscopy, we propose an electron-counting model that accounts for these differences. The model also predicts that unintentional defects and intentional dopants can create local spin moments at Si(*hkk*)-Au step edges. We analyze in detail one of these predictions and verify it experimentally. This finding opens the door to using techniques of surface chemistry and atom manipulation to create and control silicon spin chains.

Understanding how magnetism arises in materials without *d* electrons poses a scientific challenge for both theory and experiment. Such an understanding also offers a tantalizing technological goal, namely the integration of semiconductor properties and nonvolatile magnetism in a single material system. One path toward this goal, based on dilute magnetic semiconductors, has developed over the past two decades. Another approach is much more recent, and exploits instead specific features of the underlying crystal structure of the semiconductor. For example, in both carbon and silicon the electronic properties of orbitals not in covalent bonds—that is, partially filled “dangling bond” orbitals—can give rise under certain circumstances to magnetic states. These states, and the particular conditions that lead to magnetism, are just beginning to be investigated systematically.

Carbon graphene nanoribbons provide a prominent example of magnetic states at the unpassivated edge of an otherwise non-magnetic material [1–4]. For silicon the situation is more complicated. Extended graphitic silicon “ribbons” do exist and indeed form by self-assembly on stepped silicon substrates. The unpassivated edges of these graphitic steps are, in some cases, spin-polarized and perhaps even magnetically ordered at very low temperature. The best studied such example is Si(553)-Au, a stepped surface created when a submonolayer amount of gold is incorporated into the first atomic layer of a silicon substrate [5]. At low temperatures the step edges of Si(553)-Au develop a tripled periodicity which is now understood to arise from the complete spin polarization of every third dangling bond along the step edge [6–12].

The Si(553)-Au system is one member of a family of Au-stabilized Si surfaces miscut from (111) toward or away from the (001) direction. This family is hence collectively denoted as Si(*hkk*)-Au. Each member of the

family (four are known and others may well exist) is built from the small set of recurring structural motifs depicted in Figure 1. Each has a basic terrace-plus-step structure. The step edge is always a single-honeycomb graphitic strip of silicon. The terrace width varies according to the Miller index (*hkk*). A chain of gold atoms, either one or two atoms wide, is incorporated on each terrace. For sufficiently wide terraces a row of silicon adatoms is also present. Notwithstanding these strong familial similarities, the individual members of the family differ in one important respect: the step edges of *some* members form spin chains—and hence may order magnetically at low temperature—while others do not.

In this Letter, we use scanning tunneling microscopy (STM) and density-functional theory (DFT) to develop a physically transparent picture explaining the formation of local spin moments in the family of Si(*hkk*)-Au surfaces. Specifically, we explain under which conditions spin chains are formed at the step edges of particular silicon (*hkk*) orientations. We use the term *spin chain* to mean a linear array of local magnetic moments with a high degree of positional order, well-defined periodicity, and non-negligible interaction between the spins. The question of whether such a spin chain becomes magnetically ordered is a separate one, which we defer to later investigation. Our detailed analysis allows us to suggest chemical pathways, such as the use of dopants, to control formation or suppression of local spin moments, which are a prerequisite for spin chains to form. As an example we demonstrate that a common native defect—a surface vacancy—creates a single spin at the step edge.

We develop our picture in several stages. (1) We use STM and DFT to propose the first detailed structural model for Si(775)-Au, a gold chain system closely related to the previously studied systems Si(553)-Au and Si(557)-Au. (2) We demonstrate that although the

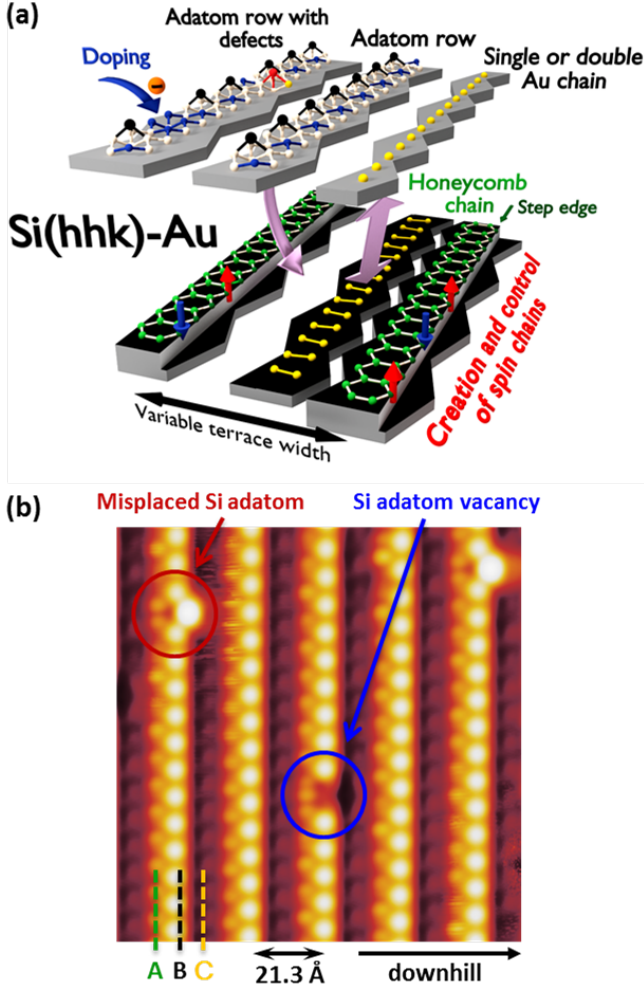


**Figure 1.** (a) Overview of the important structural motifs that control the formation of spin chains at the silicon honeycomb step edges (green hexagons) of  $\text{Si}(h\bar{h}k)$ -Au surfaces. Different crystallographic orientations ( $h\bar{h}k$ ) alter the terrace width, which leads to variations in the width of the Au chain (single or double) and to the presence or absence of additional rows of Si adatoms, which in turn open the door to adatom defects. The Au chains, Si adatoms, and defects collectively determine the electronic configuration of the silicon dangling bonds at the step edge, and hence governs the formation or suppression of local spin moments. (b) Topographic STM image of empty states on  $\text{Si}(775)$ -Au at 77 K, 150 pA, +1.0 V. Three distinct rows (A, B, C) are labeled. Two common native defects are labeled and discussed in the text.

atomic structure of  $\text{Si}(775)$ -Au is very similar to those earlier systems, the atoms comprising its step edge are *not* spin-polarized, and hence that spin chains are not formed on  $\text{Si}(775)$ -Au. (3) We provide experimental evidence supporting a theoretical prediction, made previously, that every second atom along the step edges of  $\text{Si}(557)$ -Au is spin-polarized [9], and hence that spin chains do form on  $\text{Si}(557)$ -Au. (4) We propose an electron counting model that explains these findings and use this model to predict that atoms at the  $\text{Si}(775)$ -Au

step edge become spin-polarized when holes are added to the system. (5) We identify a specific, commonly observed native defect on  $\text{Si}(775)$ -Au which creates holes in the system and, indeed, renders the adjacent step edge atom spin-polarized. Our findings open the door to using surface chemistry—that is, depositing specific atoms or molecules on the surface—in order to create, enhance, or suppress spin chains in  $\text{Si}(h\bar{h}k)$ -Au systems.

**Background and Preliminaries.** Before turning to the family of complex high-index  $\text{Si}(h\bar{h}k)$ -Au surfaces sketched in Figure 1a, we first set the stage by introducing a concept which is key to understanding silicon spin chains. We consider the electronic structure of the unusual graphitic honeycomb ribbon which forms the step edge of all known  $\text{Si}(h\bar{h}k)$ -Au surfaces. This ribbon was first addressed theoretically in Ref. 13, where it was introduced as the “honeycomb” of the honeycomb chain-channel  $3\times 1$  reconstruction of  $\text{Si}(111)$ - $M$ , where  $M$  is a metal adsorbate. When this metal is an alkali element the system is a normal band insulator. This is because, in the language of band theory, there are exactly enough electrons (four, including one from the alkali atom) to fully occupy the two band states (denoted  $S_2^+$  and  $S_2^-$ ) formed from the two  $sp^3$  orbitals belonging to the two outer atoms of the honeycomb. In the language of dangling bond orbitals, this is equivalent to saying that both of the outer atoms have doubly occupied “lone pairs” of electrons. The basic electronic configuration of the honeycomb in  $\text{Si}(111)$ - $M$  is hence insulating and non-spin-polarized.

This same basic electron configuration also describes the “ideal” step edge of  $\text{Si}(h\bar{h}k)$ -Au surfaces—that is, before any electron transfer to or from the terrace occurs. Indeed, our DFT calculations show that the Au atom plays the role of the alkali atom by donating one electron to the honeycomb step-edge states. Hence we arrive at the conclusion that the basic electronic configuration of the  $\text{Si}(h\bar{h}k)$ -Au step edge is likewise insulating and non-spin-polarized, at least before electron transfer is taken into account. The research presented below addresses the various ways, both intrinsic and extrinsic, that electrons can be transferred out of these step-edge states. This transfer is prerequisite for the formation of silicon spin chains.

**Structural Model for  $\text{Si}(775)$ -Au.** The formation of local spin moments at the steps of  $\text{Si}(h\bar{h}k)$ -Au systems depends on the electronic configuration of the unpassivated atoms at the step edge. Thus we begin by exploring an issue central to step-edge magnetism: how many electrons are available to occupy these orbitals? The answer is found on the terrace and, in particular, in the structural motifs appearing there. Wide terraces have more motifs, narrow terraces have fewer. The width of the terrace is determined by the Miller index of the surface. This index ( $h\bar{h}k$ ) can always be written in the form  $(h, h, h \pm 2n)$  where  $n$  is an integer. The unit cell period

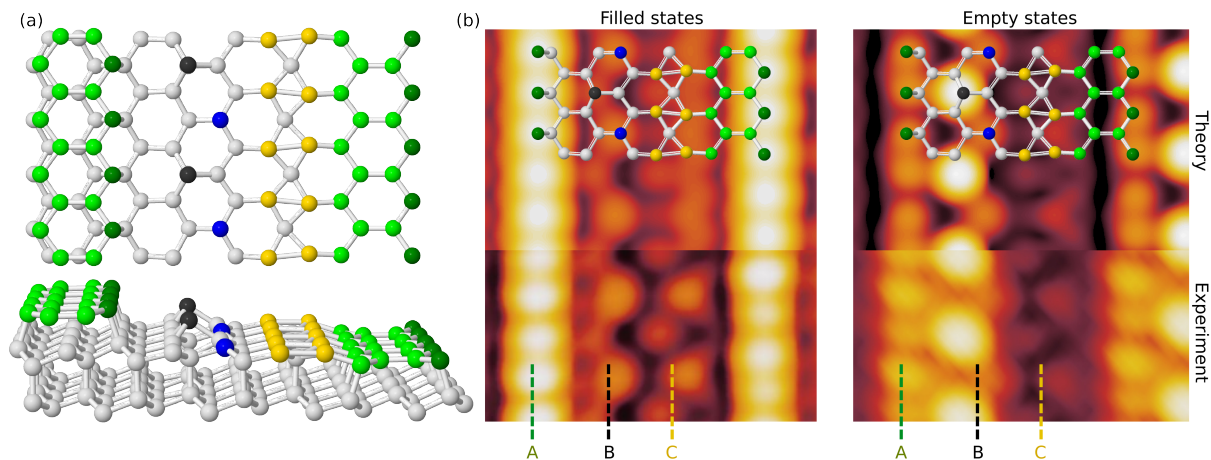


**Figure 2.** (a) Proposed structure of Si(775)-Au. Yellow atoms are Au, all others are Si. Each terrace contains a Au double row and a graphitic Si honeycomb chain (green) at the step edge. The ladder structure of the Au row has doubled ( $2a_0$ ) periodicity due to an alternating twist of the ladder rungs. A row of Si adatoms (black) with  $2a_0$  periodicity passivates three surface dangling bonds per  $1 \times 2$  cell, leaving one unpassivated Si restatom (blue) per  $1 \times 2$  cell. All of these effects give rise to discernible features in the STM topography. (b) Comparison of experimental (lower) and simulated (upper) STM images for filled and empty states (experimental bias  $-1.0$  and  $+1.0$  eV, theoretical bias  $-0.8$  and  $+0.8$  eV). Topographic features are discussed in the text. Rows A, B, and C are marked as in Figure 1b and also denote the locations at which the spectra in Figure 3a were acquired.

$L$  is then given, in units of the silicon lattice constant, by  $L^2 = S^2 + T^2$  where  $S = |h - k|/2\sqrt{3}$  is the step height and  $T = (2h/3 + k/3)\sqrt{3/8}$  is the terrace width. It is hence evident that for surface orientations close to (111), larger values of  $h$  and  $k$  correspond to wider terraces.

The terraces on Si(775)-Au are thus relatively wide,  $T = 21.1$  Å, half again as wide as on Si(553)-Au. This additional space is equivalent to two additional silicon unit cells and hence opens the door to structural motifs not found on Si(553)-Au. We turn first to the task of identifying these motifs using STM topographic imagery and DFT calculations. The resulting structural model for Si(775)-Au will then allow us to address in detail the electronic configuration—and thus the issue of magnetism—at the step edge.

Figure 1b shows a constant-current STM image of the Si(775)-Au surface. This image reveals three rows of features (A, B, C) separated by  $21.3$  Å, as well as occasional random defects which we identify as Si-adatom vacancies and misplaced Si adatoms. The three rows each show a doubled periodicity with respect to the silicon surface lattice constant  $a_0 = 3.84$  Å. These  $1 \times 2$  patterns do not change, within any row, in the temperature range studied (between 5 K and 300 K; see Supporting Information Figure S1). Hence there is no transition to higher order periodicity, in contrast to the case of Si(553)-Au [6, 7, 14]. These images are also consistent with previous STM investigations [5, 15], although improved resolution now provides tighter constraints on a detailed atomic model.

Figure 2a presents our proposed structural model of Si(775)-Au. All of the motifs are taken from Figure 1a.

The step edge is a graphitic Si honeycomb chain, just as for all other members of this family. On the terrace, a double chain of Au atoms occupies the topmost Si layer and repairs the surface stacking fault created by the graphitic chain. Hence the remainder of the terrace has a standard Si(111) crystal structure. The bare Si(111) surface would be energetically costly because of its high density of dangling bonds and thus, on extended regions, reconstructs in the well-known dimer-adatom-stacking-fault pattern. Such a reconstruction is not possible on Si(775)-Au and hence this (111)-like region simply incorporates Si adatoms to passivate most of its surface dangling bonds. This creates a staggered double row of alternating adatoms and unpassivated “restatoms” with  $1 \times 2$  periodicity.

Figure 2b compares theoretically simulated STM images for this structural model to high-resolution experimental data. The agreement is excellent in both the filled- and empty-state images and allows us to identify the atomic origin of all experimentally observed features. The bright rows visible in the occupied states, labeled A in Figure 1, arise from the unpassivated atoms at the edge of the graphitic step. The zigzag row just to the right of this step, labeled B in Figure 1, arises from the staggered row of adatoms and restatoms. The experimental bias dependence of both rows is striking and in excellent agreement with theory: row A is bright in filled states and weak in empty states, while in row B different parts of the zigzag chain are highlighted by reversing the bias—the restatoms are brightest in filled states, while the adatoms dominate the empty states.

Dimerization of the Au double row gives rise in STM to a double row of staggered spots. Specifically, a  $1 \times 2$  periodicity within each of the two rows is created because the rungs of the Au ladder twist with alternating sign along the row [16]. Row C arises from the right-hand leg of the ladder formed by the Au chain. An additional row of weak spots, between rows B and C, arises from the left-hand leg in similar fashion.

In summary, the detailed structure, spacing, periodicity, and bias dependence of all the features observed experimentally by STM on Si(775)-Au are accurately explained by our proposed structural model.

### Absence of Spin Polarization in Si(775)-Au.

Having established a plausible complete atomic model for Si(775)-Au, we turn now to its electronic structure. Our main theoretical finding is that the step edge is completely non-spin-polarized within DFT. This is perhaps surprising, especially in light of the many structural similarities to Si(553)-Au, for which every third step-edge atom is completely spin-polarized. The reason for this difference is that there are enough electrons available to completely fill all the dangling-bond orbitals at the Si(775)-Au step edge, thus forming doubly occupied lone pairs with zero spin polarization. We will return to this point below.

Experimentally, we used scanning tunneling spectroscopy (STS) with a lock-in technique to obtain a direct measurement of the local electronic states at the step edge. Figure 3a shows scanning tunneling spectroscopy (STS)  $dI/dV$  spectra taken at the locations marked in Figure 2b. The spectrum taken at the step edge is strongly peaked at  $-0.8$  eV and has no significant weight above the Fermi level. This is the signature of a fully occupied state and is hence consistent with the theoretical result of a non-spin-polarized lone pair at the Si(775)-Au step edge.

These findings are strikingly different from those for Si(553)-Au. In that case, previous DFT calculations predicted the existence of an unoccupied electronic state localized at the step edge and several tenths of an eV above the Fermi level [9]. This state was subsequently observed in STS measurements [11, 12, 17] and may be considered the experimental fingerprint for a spin-polarized step-edge state. The absence of such a fingerprint for Si(775)-Au calls for an explanation of this difference. We will turn to this explanation below. But first we present results for one more family member, Si(557)-Au.

**Experimental Evidence for Spin Polarization in Si(557)-Au.** The Si(557)-Au surface offers an interesting crystallographic contrast to those on Si(553)-Au and Si(775)-Au, because its steps are oriented oppositely [5]. A complete structural model has already been published and is largely consistent with earlier X-ray data [18, 19]. This model is again composed entirely of structural motifs from Figure 1a. Notwithstanding its different crystallographic orientation, the step edge is again a single-

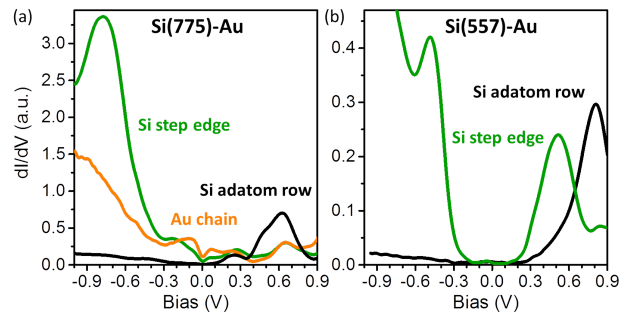


**Figure 3.** (a) Scanning tunneling spectroscopy (STS) spectra taken at the three different structural elements of the Si(775)-Au surface at 77 K. Several single-point spectra were averaged to reduce statistical noise. (b) STS spectrum from the Si(557)-Au surface at the same temperature and location as in (a). In contrast to Si(775)-Au, there is an intense feature at 0.5 V above the Fermi level—evidence for spin polarization at the step edge. Note that both panels show a peak from the adatom row at 0.6–0.8 eV, which originates from the empty dangling-bond orbital. The smaller peaks observed in panel (a) from the Si step edge and the Au chain in this energy region arise from the finite spatial resolution of the STM tip. These spectra are in good qualitative agreement with local densities of states predicted by DFT; see Figure S2 in the Supporting Information.

honeycomb graphitic strip of silicon. Despite the similarity of its Miller index to (775), the reversed orientation implies a shorter terrace,  $T = 18.8$  Å. Hence the Si(557) terrace can only accommodate a single Au chain, which does not dimerize. The remainder of the terrace is identical to that of Si(775)-Au, consisting of a staggered double row of adatoms and restatoms.

The theoretically predicted ground state of Si(557)-Au, already reported [9], shows that every second dangling bond on the step edge is only singly occupied and hence fully spin polarized. This ordering of the charge does not by itself induce  $1 \times 2$  periodicity, because the adatom-restatom row already does this. For this reason, Si(557)-Au does not undergo any structural transitions at low temperature to higher order periodicity. In contrast, for the case of Si(553)-Au the experimental observation of such a transition (to tripled periodicity) constituted the first compelling evidence for the existence of spin chains in that system [6, 7, 9]. Because Si(557)-Au does not exhibit this transition, the experimental confirmation of spin chains in Si(557)-Au must rely on a different approach.

Here we present experimental evidence that supports the theoretical prediction of an unoccupied state, at several tenths of eV above the Fermi level, arising from spin polarization of a step-edge atom on Si(557)-Au. Figure 3b shows the  $dI/dV$  spectrum from the step edge. A well-defined state at 0.5 eV above the Fermi is clearly evident [20]. This is the same unoccupied dangling-bond state that was previously observed on Si(553)-Au, and



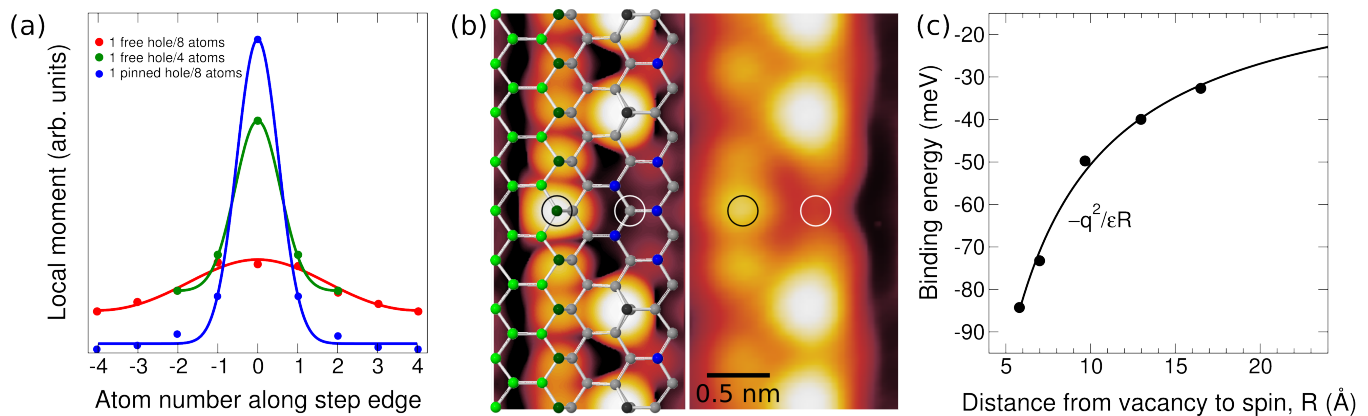


**Figure 4.** (a) Theoretically predicted formation of spin moments when holes are added to Si(775)-Au. When added at low concentrations, the resulting spins partially delocalize along the step edge; compare the cases of one free hole per 8 step-edge atoms (red) and per 4 step-edge atoms (green). Holes can also be pinned by their electrostatic attraction to a nearby charged defect [here, the adatom vacancy in panel (b)]. In this case the spin is more strongly localized (blue). Curves are Gaussian fits to DFT local magnetic moments. (b) Simulated and experimental empty-state STM images of an adatom vacancy (white circle) on Si(775)-Au. The vacancy adds one hole, which renders the nearest step-edge atom (black circle) spin-polarized and hence brighter in STM. (c) Theoretical electrostatic binding energy of the negatively charged adatom vacancy to the positively charged step-edge spin. The lowest energy configuration, with binding energy 85 meV, is realized in (b).

supports the predicted spin polarization of the step edge of Si(557)-Au.

**Spin Chains and Electron Counting.** We turn now to understanding in detail the relationship between the structural motifs on Si(*hkk*)-Au surfaces and the spin-polarization state of their steps. Each atom on the step edge forms three covalent bonds and thus has a single  $sp^3$  orbital that is not part of any bond. To a first approximation—neglecting band dispersion—this orbital can be occupied by either zero, one, or two electrons (as a lone pair). DFT results for all known Si(*hkk*)-Au surfaces show one-electron occupancy always occurs with a large on-site exchange splitting (of order 1 eV) irrespective of any magnetic order in the system. This leads to our principal finding: *the condition for forming local spin moments is that the electron count is large enough to singly occupy some, but not large enough to doubly occupy all, of the step-edge orbitals.* On Si(553)-Au, two-thirds of the orbitals are doubly occupied and one-third are singly occupied, forming spin chains with period  $3a_0$ . On Si(557)-Au, one-half are doubly occupied and one-half are singly occupied, forming spin chains with period  $2a_0$ . On Si(775)-Au, every orbital is doubly occupied and so spin chains do not form.

Another interesting case is provided by a fourth system, Si(335)-Au, which has been extensively studied by other researchers. STM topographic measurements show,[21] and DFT calculations confirm,[22] that half the step-edge orbitals are doubly occupied and half are empty. DFT calculations also show that local spin moments do not form on Si(335)-Au, consistent with the condition proposed above. In the Supporting Information we show that for all four Si(*hkk*)-Au surfaces these

step-edge occupancies, which were obtained from DFT calculations, can also be easily derived using simple electron counting.

Of course, one might ask why Si(335)-Au does not instead form a spin chain with both atoms singly occupied. This scenario might appear plausible because energy is gained by the exchange splitting of the singly occupied atoms. But there is a large Coulomb energy penalty for having *adjacent* atoms spin-polarized; this was previously discussed in a theoretical investigation of finite-temperature dynamics of the spins on Si(*hkk*)-Au. [14] Hence this hypothetical scenario is energetically forbidden.

The completely non-polarized step of Si(775)-Au provides an interesting test case for the notion of creating and manipulating spins in Si(*hkk*)-Au more generally. Our picture of electron counting suggests that if one adds holes to Si(775)-Au then local spin moments would be created there, provided that the holes localize at the step edge and not somewhere else. Figure 4 demonstrates and illuminates this result in several ways. We begin by adding holes to the ideal Si(775)-Au system and analyzing their effect. Our findings are as follows. (1) The holes indeed completely localize at the step edge. (2) Local magnetic moments develop at step-edge atoms, with the total moment equal to the number of added holes. (3) These spin moments are partially delocalized along the step edge, as shown in Figure 4a. (4) The degree of spin delocalization depends on the hole concentration, unless charged pinning defects are present. In that case electrostatic attraction between the spin and the defect further localizes the spin along the step; we will return to this below. Based on this theoretical proof of principle, we

turn now to explicit chemical strategies for adding holes (or electrons) to Si(*hkk*)-Au surfaces and hence creating spins.

**Spin Chains and Surface Chemistry.** We propose that surface chemistry offers a potentially useful tool for creating (or suppressing) spin chains in the family of Si(*hkk*)-Au surfaces. The basic idea is to use native defects and adsorbates on the terrace to control the electronic configuration on the step edge. Gold atoms have already been used for doping Si(553)-Au to study electronic confinement [23], so it is plausible that other adsorbates will work.

The Si(775)-Au surface has several naturally occurring defects with a surface concentration of 5 to 10%. Here we demonstrate that one of these defects—a missing Si adatom from row B—creates one spin at the step edge. To provide an intuitive understanding of this result we first count electrons. Each adatom brings four electrons to the surface. Three of these are used to form covalent bonds from the three surface dangling bonds that surround the adatom site. Our analysis shows that the single surface orbital of the adatom itself is empty. Thus the fourth electron must reside elsewhere. Our DFT calculations show that this electron goes to the nearest available orbital on the step edge, creating a doubly occupied lone pair. With this understanding in hand we now reverse the analysis and obtain the following fundamental result: creating an adatom vacancy removes one electron from a doubly occupied step edge orbital. In DFT a singly occupied step-edge orbital is fully spin polarized. Hence each adatom vacancy creates one spin at the step edge.

Experimental evidence indeed supports this analysis. Figure 4b shows a DFT-simulated STM image of the region around an adatom vacancy. The nearest step-edge atom is now spin-polarized, which increases its intensity when imaged at positive bias because the single unoccupied state is above the Fermi level. The experimental STM image shows exactly this local enhancement of the nearest step-edge atom; see Supporting Information Figure S3 for a bias-dependent analysis.

Each spin created in this way is positively charged relative to the background of non-spin-polarized step-edge atoms. It follows by electroneutrality of the overall system that each adatom vacancy is negatively charged. Hence we expect an electrostatic attraction  $-q^2/\epsilon R$  between the vacancy and the spin. We tested this hypothesis theoretically by forcing the spin to localize on several nearby step-edge atoms (which it does metastably) and then computing the change in the DFT total energy relative to the case of large separation. The resulting binding energy curve, shown in Figure 4c, confirms the hypothesis. Our experimental STM results are also consistent with this attractive interaction: Figure 4b shows that the spin indeed localizes at the step edge atom closest to the adatom vacancy. We anticipate that for a group of such artificially created spins, the lowest energy configuration

will depend on the distribution of adatom vacancies and the shape of the resulting electrostatic landscape.

In addition to adatom vacancies, two other defects are commonly found on Si(775)-Au. Both are misplaced Si adatoms located one unit cell to the right of the normal position. The first creates a phase shift of the adatoms by  $a_0$  along the row, while the second does not. Electron counting shows that these defects are electron-donating and charge neutral, respectively (see Supporting Information Figure S4). Thus these misplaced-adatom defects do not create step-edge spins but rather destroy them. DFT calculations confirm, and STM images are consistent with, this prediction; see the discussion accompanying Supporting Information Figure S4.

This general model of spin creation and destruction by hole and electron doping, respectively, motivates our proposal for using surface chemistry to create and manipulate spin chains. For example, one can envision using atom manipulation techniques to create and arrange adatom vacancies on Si(775)-Au, and hence to construct spin chains with tunable lengths and spacings. In addition to the native defects discussed here, a large class of foreign adsorbates offers broad opportunities—depending on their electronic character—for inducing or suppressing step-edge spins at Si(*hkk*)-Au surfaces.

Finally, it is likely that our results and proposal for controlling spins at the steps of Si(*hkk*)-Au are also relevant—probably with interesting modifications—to many other related materials systems, such as silicene or germanene [24–27], as well as to other physical configurations, such as finite ribbons.

## Methods

**Experimental.** The *n*-doped (phosphorus) Si(775) and Si(557) substrates were cleaned by direct current heating up to 1260 °C. During Au evaporation (0.32 ML for Si(775)-Au and 0.18 ML for Si(557)-Au) the sample was held at 650 °C. In contrast to Si(553)-Au [28] post-annealing was not necessary. Successful preparation was checked with low-energy electron diffraction. High-resolution STM and STS measurements were performed with a commercial Omicron low-temperature STM at a sample temperature of 77 K. Spectroscopy data were obtained via the lock-in detection method using a modulation voltage of 10 meV (20 meV for Si(557)-Au data) at a frequency of 789 Hz. Lock-in  $dI/dV$  spectra have been offset-corrected using simultaneously recorded  $I(V)$  curves as a reference.

**Theoretical.** First-principles total-energy calculations were used to determine the relaxed equilibrium geometry and electronic properties of the structural model for Si(775)-Au. The calculations were performed using a hydrogen-passivated slab with four silicon double layers plus the reconstructed top surface layer and a vacuum region of at least 10 Å. All atomic positions were

relaxed, except the bottom Si layer and its passivating hydrogen layer, until the largest force component on every atom was below 0.02 eV/Å. Total energies and forces were calculated within the generalized-gradient approximation of Perdew, Burke, and Ernzerhof [29] to DFT using projector-augmented wave potentials as implemented in VASP [30]. Results obtained using the local-density approximation (LDA) are very similar. In the Supporting Information we also show theoretical results for the local density of states of Si(775)Au and Si(557)Au, calculated using the Heyd-Scuseria-Ernzerhof (HSE) hybrid functional. [31, 32] The plane-wave cutoff for all calculations was 350 eV. The sampling of the surface Brillouin zone was chosen according to the size of the surface unit cell; for the  $1 \times 2$  reconstruction of Si(775)-Au shown in Figure 2a we used  $2 \times 4$  sampling. Simulated STM images were created using the method of Tersoff and Hamann [33]. Spin-polarization, but not spin-orbit coupling, was included in all the calculations.

## Notes

The authors declare no competing financial interest.

Supporting Information Available: Detailed discussions of (1) electron counting of silicon step-edge occupancies on Si(*hkk*)-Au; (2) misplaced Si-adatom defects and their role in electron transfer. Also included are four additional figures with STM images and theoretical densities of states.

## Acknowledgements

The authors thank F.J. Himpsel for many helpful discussions. This work was supported by Deutsche Forschungsgemeinschaft (through Grants SFB 1170 “TocoTronics” and FOR 1700) and the Office of Naval Research through the Naval Research Laboratory’s Basic Research Program (SCE). Computations were performed at the DoD Major Shared Resource Centers at AFRL.

- 
- [1] G. Z. Magda, X. Jin, I. Hagymasi, P. Vancso, Z. Osvath, P. Nemes-Incze, C. Hwang, L. P. Biro, and L. Tapasztó, *Nature* **514**, 608 (2014).
  - [2] Y. Li, Z. Zhou, P. Shen, and Z. Chen, *ACS Nano* **3**, 1952 (2009).
  - [3] T. B. Martins, A. J. R. da Silva, R. H. Miwa, and A. Fazzio, *Nano Letters* **8**, 2293 (2008).
  - [4] C.-K. Yang, J. Zhao, and J. P. Lu, *Nano Letters* **4**, 561 (2004).
  - [5] J. N. Crain, J. L. McChesney, F. Zheng, M. C. Gallagher, P. C. Snijders, M. Bissen, C. Gundelach, S. C. Erwin, and F. J. Himpsel, *Phys. Rev. B* **69**, 125401 (2004).
  - [6] J. R. Ahn, P. G. Kang, K. D. Ryang, and H. W. Yeom, *Phys. Rev. Lett.* **95**, 196402 (2005).
  - [7] P. C. Snijders, S. Rogge, and H. H. Weitering, *Phys. Rev. Lett.* **96**, 076801 (2006).
  - [8] M. Krawiec, *Phys. Rev. B* **81**, 115436 (2010).
  - [9] S. C. Erwin and F. Himpsel, *Nat. Commun.* **1**, 58 (2010).
  - [10] W. Voegeli, T. Takayama, T. Shirasawa, M. Abe, K. Kubo, T. Takahashi, K. Akimoto, and H. Sugiyama, *Phys. Rev. B* **82**, 075426 (2010).
  - [11] P. C. Snijders, P. S. Johnson, N. P. Guisinger, S. C. Erwin, and F. J. Himpsel, *New Journal of Physics* **14**, 103004 (2012).
  - [12] J. Aulbach, J. Schäfer, S. C. Erwin, S. Meyer, C. Loho, J. Settelein, and R. Claessen, *Phys. Rev. Lett.* **111**, 137203 (2013).
  - [13] S. C. Erwin and H. H. Weitering, *Phys. Rev. Lett.* **81**, 2296 (1998).
  - [14] S. C. Erwin and P. Snijders, *Phys. Rev. B* **87**, 235316 (2013).
  - [15] L. Pedri, L. Toppozini, and M. Gallagher, *Surface Science* **601**, 924 (2007).
  - [16] The magnitude of this dimerization is sensitive to the choice of DFT exchange-correlation functional and to the silicon lattice constant. We find using PBE that the dimerization parameter  $d = (a_1 - a_0)/a_0$  has the value 0.08.
  - [17] I. Song, J. S. Goh, S.-H. Lee, S. W. Jung, J. S. Shin, H. Yamane, N. Kosugi, and H. W. Yeom, *ACS Nano* **9**, 10621 (2015).
  - [18] D. Sánchez-Portal, J. D. Gale, A. García, and R. M. Martin, *Phys. Rev. B* **65**, 081401 (2002).
  - [19] I. K. Robinson, P. A. Bennett, and F. J. Himpsel, *Phys. Rev. Lett.* **88**, 096104 (2002).
  - [20] The small spacing and STM-broadened appearance of the half-filled dangling-bond orbitals make it technically infeasible to separately resolve the spectra for the two adjacent silicon atoms.
  - [21] M. Krawiec, T. Kwapinski, and M. Jalochowski, *physica status solidi (b)* **242**, 332 (2005).
  - [22] M. Krawiec, *Surface Science* **609**, 44 (2013).
  - [23] I. Song, D.-H. Oh, H.-C. Shin, S.-J. Ahn, Y. Moon, S.-H. Woo, H. J. Choi, C.-Y. Park, and J. R. Ahn, *Nano Letters* **15**, 281 (2015).
  - [24] B. Lalmi, H. Oughaddou, H. Enriquez, A. Kara, S. Vizzini, B. Ealet, and B. Aufray, *Applied Physics Letters* **97**, 223109 (2010).
  - [25] A. Fleurence, R. Friedlein, T. Ozaki, H. Kawai, Y. Wang, and Y. Yamada-Takamura, *Phys. Rev. Lett.* **108**, 245501 (2012).
  - [26] B. Feng, Z. Ding, S. Meng, Y. Yao, X. He, P. Cheng, L. Chen, and K. Wu, *Nano Letters* **12**, 3507 (2012).
  - [27] M. E. Dvila, L. Xian, S. Cahangirov, A. Rubio, and G. L. Lay, *New Journal of Physics* **16**, 095002 (2014).
  - [28] J. N. Crain, A. Kirakosian, K. N. Altmann, C. Bromberger, S. C. Erwin, J. L. McChesney, J.-L. Lin, and F. J. Himpsel, *Phys. Rev. Lett.* **90**, 176805 (2003).
  - [29] J. P. Perdew, K. Burke, and M. Ernzerhof, *Phys. Rev. Lett.* **77**, 3865 (1996).
  - [30] G. Kresse and J. Furthmüller, *Phys. Rev. B* **54**, 11169 (1996).
  - [31] J. Heyd, G. E. Scuseria, and M. Ernzerhof, *The Journal of Chemical Physics* **118**, 8207 (2003).
  - [32] J. Heyd, G. E. Scuseria, and M. Ernzerhof, *The Journal of Chemical Physics* **124**, 219906 (2006).
  - [33] J. Tersoff and D. R. Hamann, *Phys. Rev. B* **31**, 805 (1985).

## Spin Chains and Electron Transfer at Stepped Silicon Surfaces

### 1. Electron counting of silicon step-edge occupancies on Si(*hkk*)-Au surfaces

In the main text we gave the results of DFT calculations for the silicon step-edge occupancies on four Si(*hkk*)-Au surfaces as follows:

On Si(553)-Au, two-thirds of the orbitals are doubly occupied and one-third are singly occupied, forming spin chains with period  $3a_0$ . On Si(557)-Au, one-half are doubly occupied and one-half are singly occupied, forming spin chains with period  $2a_0$ . On Si(775)-Au, every orbital is doubly occupied and so spin chains do not form. On Si(335)-Au, one-half the step-edge orbitals are doubly occupied and one-half are empty and so spin chains do not form. These results are summarized in this table:

Surface	Individual occupancies	Average occupancy
Si(335)-Au	2, 0	1
Si(557)-Au	2, 1	$3/2$
Si(553)-Au	2, 2, 1	$5/3$
Si(775)-Au	2	2

Here we show how the average occupancies can be easily obtained using simple electron counting. From these average occupancies it is straightforward to deduce the individual occupancies—and hence both the existence and period of spin chains on arbitrary Si(*hkk*)-Au surfaces.

In the *Background and Preliminaries* section of the main text, we showed that the hypothetical “ideal” step edge of Si(*hkk*)-Au surfaces—that is, before any electron transfer to or from the terrace occurs—consists of doubly occupied lone pairs on every silicon step-edge atom. This result was obtained by considering the electronic structure of Si(111)-*M* surfaces (where *M* is an alkali), for which there is no step. When a step and terrace are introduced the electron counting is slightly more complicated. In the following we apply this counting to the four surfaces in the table.

We begin with the simplest system, Si(335)-Au, which has the smallest possible terrace, consisting of a single silicon row. Each atom in this row has two dangling bonds which combine to form two bands, one bonding and one antibonding. The bonding band is completely filled and the antibonding band (which has parabolic dispersion and is traditionally called the “Au band”) is approximately half-filled in DFT calculations; hence a total of three electrons is required. Two come from the singly occupied dangling bonds themselves and one from the Au atom. Because the Au electron is no longer available to occupy the step-edge orbital, this reduces the occupancy of the step-edge orbital from two to one. Hence the average occupancy of a Si(335)-Au step-edge orbital is 1.

The Si(557)-Au surface is slightly more complicated because it contains, in addition to the features of Si(335)-Au, one row of silicon adatoms with  $1 \times 2$  periodicity. In the main text it was shown that each such adatom adds one electron to the system. Hence, because there is one adatom for every two step-edge atoms, the average occupancy of a Si(557)-Au step-edge orbital is  $1/2$  more than for Si(335)-Au, that is,  $3/2$ .

The last two surfaces, Si(553)-Au and Si(775)-Au, are still more complicated because the Au chain is now double rather than single. Si(553)-Au has no adatoms and, aside from the double Au chain, is structurally equivalent to Si(335)-Au. Thus we begin the electron counting from that reference point. Each Au atom in the second chain breaks an intact Si bond on the terrace of the Si(335)-Au surface, leaving a row of Si dangling bonds which form another parabolic “Au band” which is one-sixth filled; hence one-third of an electron is required. The Au electron is needed to passivate another surface Si dangling bond created at the bottom of the step edge, and thus the required one-third electron must come from the electron in the terrace-Si dangling bond. This leaves two-thirds of an electron left over to occupy the step-edge orbital. Hence the average occupancy of a Si(553)-Au step-edge orbital is  $2/3$  more than for Si(335)-Au, that is,  $5/3$ .

We count electrons on Si(775)-Au starting from the reference state Si(557)-Au because both surfaces are, aside from the Au chain, structurally equivalent. Each Au atom in the second chain breaks an intact Si bond on the terrace of the Si(557)-Au surface, which leaves a row of Si dangling bonds to form another parabolic “Au band” which is one-fourth filled; hence one-half of an electron is required. As argued above, this must come from the electron in the terrace-Si dangling bond. This leaves one-half electron left over to occupy the step-edge orbital. Hence the average occupancy of a Si(775)-Au step-edge orbital is  $1/2$  more than for Si(557)-Au, that is, 2.



Finally, from these average occupancies we can deduce the actual individual occupancies. Two rules suffice, both explained in the main text: (1) Only integer occupancies are allowed; (2) Singly occupied orbitals cannot be adjacent. Applying these rules we find that Si(335)-Au has  $1 \times 2$  periodicity with individual occupancies (2, 0); Si(557)-Au has  $1 \times 2$  periodicity with occupancies (2, 1); Si(553)-Au has  $1 \times 3$  periodicity with occupancies (2, 2, 1); and Si(775)-Au has  $1 \times 2$  periodicity (due to the adatom row) with occupancies (2,2). These periodicities and occupancies agree with those obtained from detailed DFT calculations and are consistent with all available experimental data. Moreover, the onsite exchange splitting of singly occupied orbitals implies the existence of spin chains for Si(553)-Au and Si(557)-Au, but not for Si(335)-Au or Si(775)-Au; this is also consistent with DFT calculations and experiment.

## 2. Misplaced Si-adatom defects and electron transfer

In addition to the adatom vacancy discussed in the main text (Figure 4b), the Si(775)-Au surface hosts two other common defects namely two different types of misplaced adatoms. A structural model and simulated STM images, as well as experimental STM data for both misplaced adatom defects (Type I and Type II), are displayed in Figures S4a and b, respectively. In both cases the theoretical simulation is in detailed agreement with the experimental STM images, giving excellent support for both structural models. Defect Type I interrupts the usual  $2a_0$  spacing of normal adatoms, reducing by  $a_0$  the normal  $4a_0$  spacing between the two adjacent normal adatoms. As indicated by the colored dots and stars in the unoccupied STM images at 0.5 and 0.2 V not only the adatom row, but also the Au chain and the Si step edge atoms, exhibit this phase shift by  $a_0$  (see Figure S4a).

The effect of this native defect on the step edge's electron concentration is easiest to evaluate in three stages: As discussed in the main text, removal of a normal adatom and its four electrons from the model in Figure 2a transfers one hole to the step edge. Next we shift the entire row of normal adatoms on one side of this vacancy toward it by  $a_0$ , anticipating the actual spacing around the misplaced adatom defect. This increases by one-half the total number of adatoms. Since the addition of half an adatom is equivalent to the addition of half an electron, we have so far added 0.5 holes to the step edge. Finally, we return the adatom to its new misplaced site, passivating two silicon atoms and forming one bond to a gold atom; thus this returned adatom is again equivalent to adding one electron. Considering all three stages, we see that the overall net change created by a misplaced adatom defect is *0.5 additional electrons*. Thus, the misplaced adatom defect Type II should *not* induce any spin-polarization in the step edge atoms. This is confirmed by the experimental STM images around adatom defect Type I, which do not show any evidence of spin-polarized step-edge atoms.

For misplaced adatom defect Type II (Figure S4b) the electron counting follows the same line as for Type I. However, the  $1 \times 2$  cell lacks the additional adatom (and thus half an electron) induced by the phase shift of  $a_0$ , which occurs only for defect Type I. Therefore, defect Type II is *charge neutral* and should not induce any spin polarization on step-edge atoms. Again, this is consistent with the experimental STM results and hence confirms our description of electron transfer between native defects and the silicon step edge.

### 3. Supplementary figures

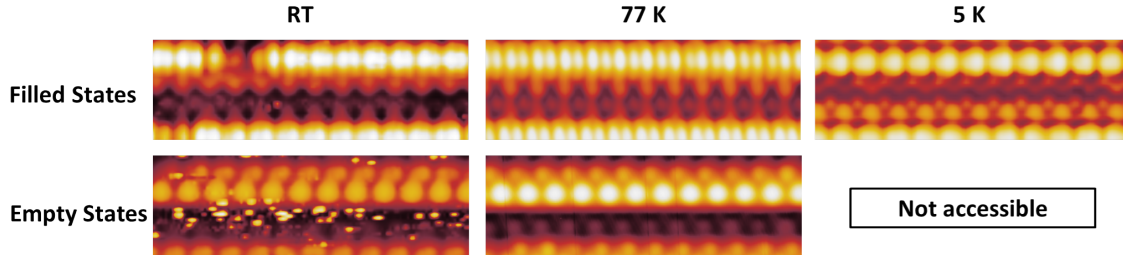


**Figure S1. Absence of a phase transition in Si(775)-Au.** Constant current STM images of the Si(775)-Au surface at various sample temperatures. Filled states images have been taken at  $U = -1.0$  V ( $U = -0.95$  V for 77 K) and empty states are shown for  $U = +1.0$  V. All three chain types, namely, the Si honeycomb row, the Si adatom row as well as the Au chain, do not change their  $\times 2$  periodicity between room temperature and 5 K, which indicates the absence of a phase transition in this temperature window.

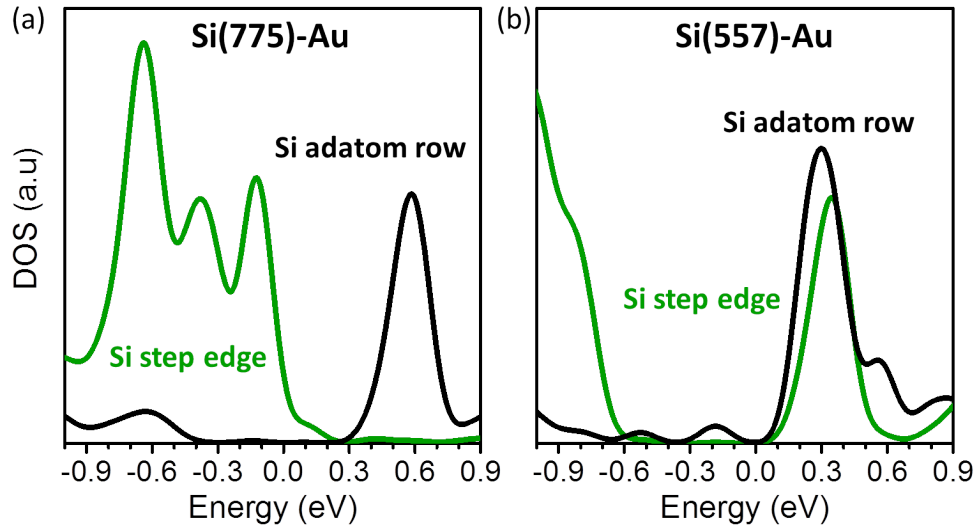


**Figure S2. Theoretical DFT/HSE local densities of states for Si(775)-Au and Si(557)-Au.** (a) For Si(775)-Au the step edge is predicted to consist of doubly-occupied lone-pairs on every atom. Hence the step-edge local density of states (LDOS) shows no states above the Fermi level; only the unoccupied orbitals of the Si adatom row appear there. (b) For Si(557)-Au the step edge is predicted to consist of alternating doubly-occupied and singly-occupied atoms. Hence the LDOS additionally shows a strong peak above the Fermi level. Both panels are in good qualitative agreement with Figure 3 of the main text.

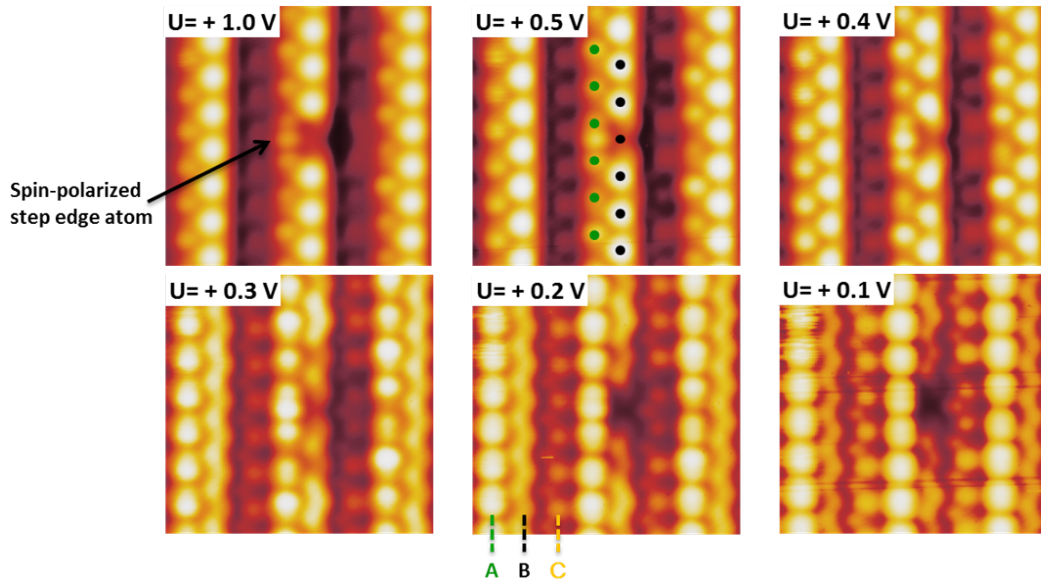


**Figure S3. Bias dependence of an adatom vacancy.** STM bias series of the Si(775)-Au unoccupied states including an adatom vacancy. The adatom vacancy dopes one hole to the step edge and thus renders the nearest step-edge atom (black arrow) spin-polarized and hence brighter in STM. The green and black dots make it clear that this vacancy does not create a phase shift of other features within the same row (in contrast to the misplaced adatom defect in Figure S4a). These images are consistent with the structural model of a vacancy shown in Figure 4b of the paper. In addition, the zigzag appearance of row B at bias  $\leq 0.3$  V, as well as the inversion of adatom vs honeycomb row relative intensities that occurs at about 0.4 V, provide additional support for our basic structural model of Si(775)-Au.

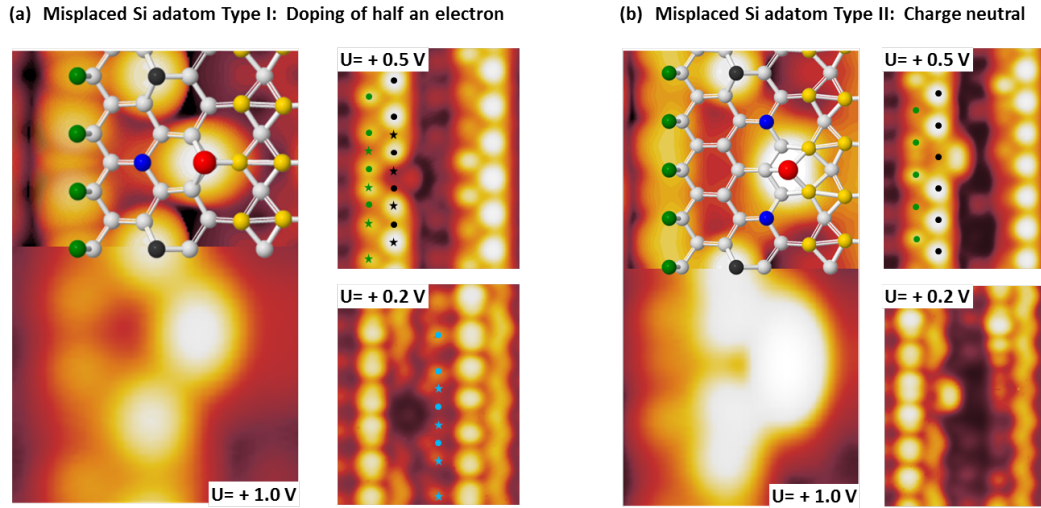


**Figure S4. Two types of misplaced-adatom defects and the resulting charge transferred to the silicon step edge.** (a) Structural model and STM imagery for Type I misplaced-adatom defect. This defect disrupts the usual adatom spacing, as indicated by the colored dots and stars in the right-hand panels. (b) Structural model and STM imagery for Type II misplaced-adatom defect. In contrast to the Type I defect, the Type II defect does not disrupt the adatom spacing, as demonstrated by the green and black dots in the right-hand panel.